

https://doi.org/10.1070/QEL17066

Investigation of an electron-beam pumped VECSEL based on an InGaAs/AlGaAs heterostructure

A.Yu. Andreev, T.A. Bagaev, M.R. Butaev, N.A. Gamov, E.V. Zhdanova, M.M. Zverev, V.I. Kozlovsky, Ya.K. Skasyrsky, I.V. Yarotskaya

Abstract. **We report the results of a study of an e-beam pumped vertical-external-cavity surface-emitting laser (VECSEL) based on an InGaAs/AlGaAs heterostructure. Metalorganic chemical vapour deposition (MOCVD) is employed to grow two structures of different design, which contain 10 quantum wells (QWs) and a built-in distributed Bragg reflector (DBR) mirror. Under repetitively pulsed electron-beam excitation (50 Hz, 250 ns), a peak output power of 5.5 W is achieved at a wavelength of 2.5 W and an output power of 2.5 W at 1.013 μm with a total convergence angle no larger than 20 mrad.**

Keywords: *VECSEL, InGaAs/AlGaAs MQW heterostructure with a DBR mirror, e-beam pumping.*

1. Introduction

A vertical-external-cavity surface-emitting laser (VECSEL), or a semiconductor disk laser (SDL), has been vigorously studied since the first publication by Kuznetsov et al. [1] in 1997, who employed for the first time a heterostructure with resonant periodic gain pumped with the radiation of a laser diode. Numerous applications of these lasers arise from the high beam quality for an output power of several watts, from the possibility of continuous wavelength tuning, and from the mastering of the topical wavelength ranges – mid-UV, visible, mid-IR, and terahertz ranges – by the nonlinear intracavity conversion of the laser frequency.

The best results with SDLs were obtained with InGaAs/GaAs quantum wells (QWs). Specifically, Heinen et al. [2] achieved a cw output power of 106 W at a wavelength close to 1.03 μm under optical pumping by diode lasers with a wavelength of 808 nm. With the use of nonlinear intracavity frequency conversion of the radiation of a SDL to the third harmonic it is possible to obtain UV radiation at a wavelength of about 350 nm [3]. Further advancement to the mid-UV range entails a significant complication of the optical configuration of the laser system [4].

An alternative approach involves the use of wide-gap InGaN/GaN heterostructures or II–VI compounds, which radiate in the blue–green spectral range, with the subsequent conversion to the second harmonic. However, since commercially available and efficient laser diodes for pumping such structures so far are nonexistent, electron-beam pumping is quite topical [5, 6]. An e-beam pumped InGaAs/GaAs heterostructure SDL was investigated in Ref. [6]. The structure was grown by molecular-beam epitaxy. In our work we present new results of similar investigations with the use of heterostructures grown by metalorganic chemical vapour deposition (MOCVD).

A.Yu. Andreev, T.A. Bagaev, I.V. Yarotskaya OJSC M.F. Stel'makh Polyus Research Institute, ul. Vvedenskogo 3, stroenie 1, 117342Moscow, Russia;
M.R. Butaev, V.I. Kozlovsky Lebedev Physical Institute, Russian Academy of Sciences, Leninsky prosp. 53, 119991 Moscow, Russia; National Research Nuclear University 'MEPhI', Kashirskoe shosse 31, 115409 Moscow, Russia; e-mail: vikoz@sci.lebedev.ru;
N.A. Gamov, E.V. Zhdanova Moscow Technological University (MIREA), prosp. Vernadskogo 78, 119454 Moscow, Russia;
M.M. Zverev Moscow Technological University (MIREA), prosp. Vernadskogo 78, 119454 Moscow, Russia; Lebedev Physical Institute, Russian Academy of Sciences, Leninsky prosp. 53, 119991 Moscow, Russia; e-mail: mzverev@mail.ru;
Ya.K. Skasyrsky Lebedev Physical Institute, Russian Academy of Sciences, Leninsky prosp. 53, 119991 Moscow, Russia

Received 23 May 2019
Kvantovaya Elektronika **49** (10) 909–912 (2019)
Translated by E.N. Ragozin

2. Characteristics of the structures

Two structures (A and B) were grown by MOCVD and contained a built-in distributed Bragg reflector (DBR) mirror of 30 $Al_{1-x}Ga_xAs/Al_yGa_{1-y}As$ layer pairs sequentially grown on an n-type GaAs substrate, 10 $In_zGa_{1-z}As/GaAs$ QWs with $GaAs_{1-u}P_u$ layers for elastic stress compensation, as well as an additional matching GaAs layer and an $Al_{0.55}Ga_{0.45}As$ layer to prevent diffusion. Structure B had an additional 6-nm thick GaAs capping layer. The x, y, z, and u composition parameters and the layer thicknesses of the structures under investigation were different and were selected in such a way as to obtain lasing near 1.02 μm (structure A) and 1.06 μm (structure B).

Figure 1 depicts the reflection and photoluminescence spectra of the resultant structures. The absolute value of the reflection coefficient was measured with an uncertainty of ±1%. A significant dip in reflectivity at a wavelength of about 1.06 μm for structure B, which is hardly different in position from the photoluminescence peak, inficates that the resonance of the microcavity formed by the structure surface and the DBR mirror coincides nicely with the QW absorption edge. For structure A, the coincidence of the peaks is somewhat worse.

3. Experiment

The laser is schematically shown in Fig. 2. Silver paste is used to attach the structure to a copper heat sink, which is accommodated in a vacuum chamber at room temperature (~20 °C). The external planoconcave SDL mirror had a radius of curvature r = 30 mm and a reflectivity of 98% at a wavelength λ = 1.015 μm and a reflectivity of 98.5% at λ = 1.06 μm. The mirror was also placed inside the vacuum chamber. The reso-

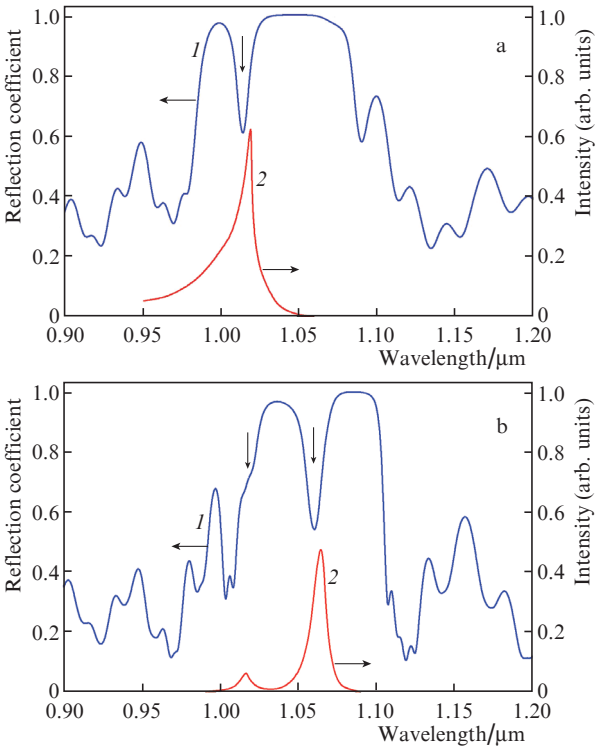

Figure 1. (*1*) Reflection and (*2*) photoluminescence spectra of structures (a) A and (b) B. Vertical arrows indicate the positions of the cavity eigenmodes of the structure.

nator length L was equal to 26 mm. The calculated diameter $2w_0$ of the fundamental mode at the structure was equal to about 80 μm. The electron beam was incident on the structure at an angle of approximately 30° and performed a pulse-periodic line scanning at a frequency of 50 Hz with a velocity $v_{sc} = 8 \times 10^4$ cm s^{-1}. The position of the line could be continuously varied in the transverse direction until one of its points coincided with the position of the resonator mode on the structure surface. The SDL radiation was extracted from the vacuum chamber through a TF-5 lead glass window with the help of a folding Au mirror. The radiation was recorded with a calibrated FEK-29 photocathode.

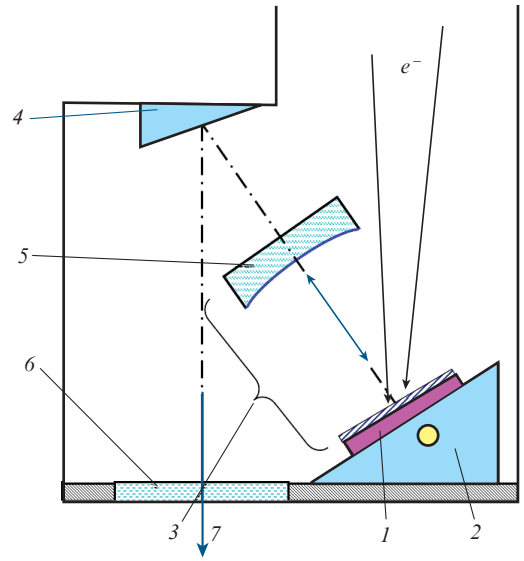

Figure 2. Laser schematic:
(*1*) semiconductor structure; (*2*) copper heat sink; (*3*) optical resonator; (*4*) folding mirror; (*5*) external output mirror; (*6*) vacuum chamber window; (*7*) laser beam; (e^-) electron beam.

4. Laser characteristics and discussion of results

Figure 3 shows the output radiation spectra of the lasers based on structures A and B. The A-structure laser spectrum peaked at a wavelength of 1.013 μm and the B-structure laser spectrum had a maximum at 1.062 μm. The half-height width of the spectrum was equal to 3.5 nm for structure A and to 0.9 nm for structure B. The spectrum of A-structure lasing was modulated with a sub-line spacing $\delta\lambda = 0.36$ nm. This modulation is supposedly caused by the additional reflection from the rear surface of the 350-μm thick GaAs growth substrate. Indeed, $\delta\lambda$ may be estimated by the formula $\delta\lambda = \lambda^2/(2HN^*)$, where $\lambda = 1.013$ μm is the oscillation wavelength, $H = 350$ μm is the GaAs substrate thickness, and $N^* \approx 4.23$ is the effective refractive index of GaAs at a wavelength of 1.013 μm with the allowance for dispersion. As a result, we have $\delta\lambda = 0.347$ nm, which is hardly different from the measured value of 0.36 nm.

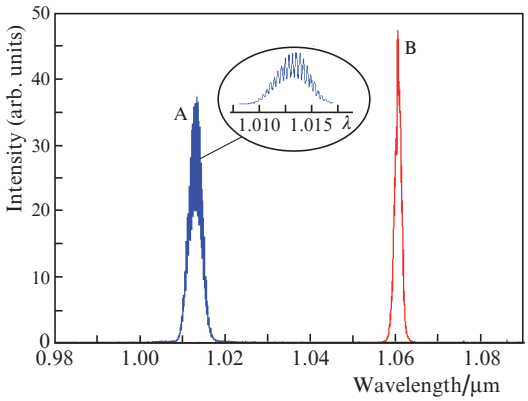

Figure 3. Lasing spectra of the A- and B-structure lasers. The inset shows the lasing spectrum of the A-structure laser with a higher resolution.

Structure B did not exhibit a similar modulation, since the second surface of its GaAs substrate was matted. Appreciable modulation of the spectrum is indication that the DBR mirror is not exactly a highly reflecting mirror and that the radiation absorption coefficient at the oscillation wavelength is low in the GaAs substrate. This comes as a surprise, since the calculated DBR mirror reflectivity at the oscillation wavelength exceeds 99.98%.

Figure 4 depicts the oscilloscope trace of the output pulse of the B-structure SDL for the highest peak power. The base pulse duration is slightly longer than 250 ns. The pulse shape and duration depended on the diameter d_e and current I_e of the electron beam. When d_e was appreciably smaller than $2w_0$, the pulse duration shortened to ~100 ns, which corresponded to the electron beam time of flight through the transverse size of the fundamental resonator mode $t_p = 2w_0/v_{sc} = 100$ ns. However, for $d_e < 2w_0$ the peak power declined. This is supposedly due to the fact that the absorption of laser radiation is rather high outside of the excitation domain.

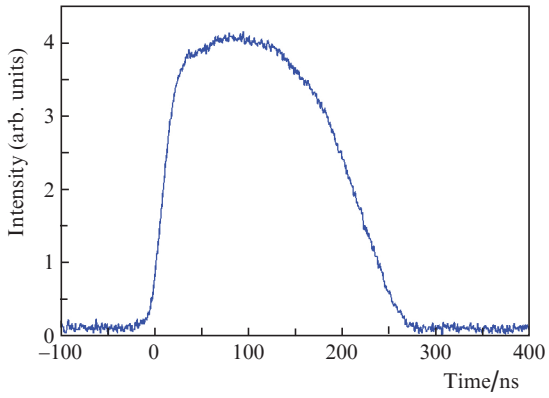

Figure 4. Oscilloscope trace of the output pulse of the B-structure SDL for a current $I_e = 1$ mA.

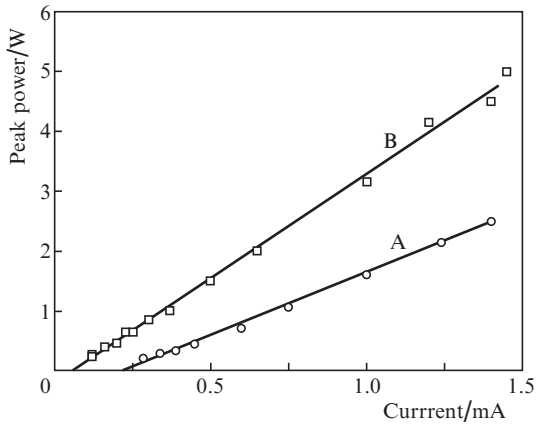

Figure 6. Peak output power of the A- and B-structure SDLs as a function of the electron beam current for an electron energy of 32 keV. The electron beam diameter was optimised for each value of I_e for maximising the peak power.

With increasing electron beam diameter, the pulse lengthens because lasing starts and terminates for an incomplete overlap of the traveling electron beam with the fundamental resonator mode. When $d_e > 2w_0$, the oscillation of higher transverse resonator modes is possible (especially for high values of I_e). In this case, t_p may lengthen up to 500 ns with a simultaneous lowering of the peak power. The far-field pattern of the B-structure SDL is depicted in Fig. 5 for different values of I_e. It was recorded with a Canon 350D digital camera without an objective at a distance of 220 mm from the structure surface. For a small overshoot of the lasing threshold, the directivity pattern has a close-to-Gaussian transverse intensity distribution. One can see in the two-dimensional pattern the rings, which arise from the radiation interference at the planoconcave substrate of the output mirror. The total radiation divergence angle was equal to 6 mrad at a level of e^{-1}. The calculated Gaussian beam divergence $\theta = \lambda/(\pi 2w_0)$ is equal to about 4 mrad. The disagreement with the experimental value is due to the radiation passage through the external mirror substrate, which is a diverging lens.

With increasing electron beam current, higher-order transverse resonator modes break into oscillation, and the total divergence angle for the peak I_e value is approximately three times higher. Observed in this case is the pattern 'stretching' in the direction parallel to the direction of electron beam scanning.

Figure 6 shows the dependence of the peak output power of the A- and B-structure SDLs on the electron beam current. The threshold current, which was determined from the linear approximation of the resultant data, was equal to 0.2 mA for the former structure and 0.06 mA for the latter one. For an electron beam diameter of 80 μm these values correspond to respective threshold current densities of 4 and 1.2 A cm^{-2}, which are comparable with the estimate (2.2 A cm^{-2}) obtained in Ref. [6].

The low-threshold B-structure laser yielded a maximum power of 5 W at a wavelength of 1.062 μm for an electron energy of 32 keV. The highest power of the other laser amounted to about 2.5 W at $\lambda = 1.013$ μm. For the A-structure laser, the threshold current was higher and the output power was lower due to a mismatch between the spacing of the QWs and the spacing of the antinodes of the resonator modes.

Figure 7a shows the dependence of the highest peak power of the B-structure SDL on the electron energy. The highest power of 5.5 W was achieved for an energy of 44 keV; with decreasing energy to 15 keV the power falls to zero. Among the factors of this fall is a lowering of the maximal current with a decrease in electron energy in our facility.

Figure 7b depicts the efficiency of this laser in relation to the electron energy. The highest efficiency is achieved for 26 keV and amounts to 10.5%. The lowering of efficiency with increasing electron energy is due to the fact that part of the electrons pass through the active structure region and is absorbed in the DBR mirror. With a decrease in electron energy, the ionisation energy loss curve 'nestles' to the structure surface and the fraction of electrons that reaches the QWs becomes smaller. The efficiency of lasing may be improved (especially for a low electron energy) by making the barrier and matching layers thinner. The first QW may be positioned at a half-wavelength distance from the structure surface.

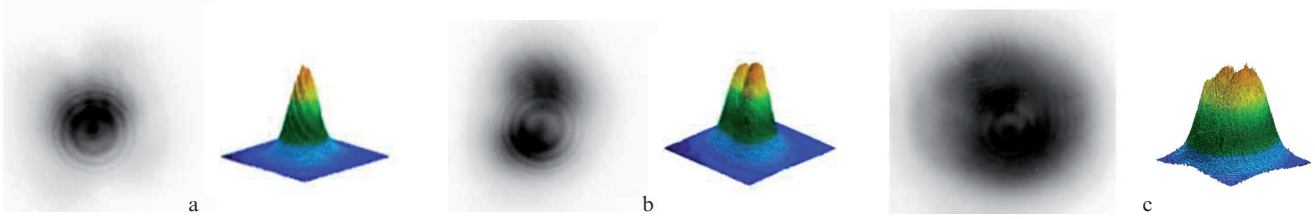

Figure 5. (Left) Two-dimensional and (right) three-dimensional far-field patterns of the B-structure SDL radiation for I_e = (a) 0.2, (b) 0.65, and (c) 1.4 mA.

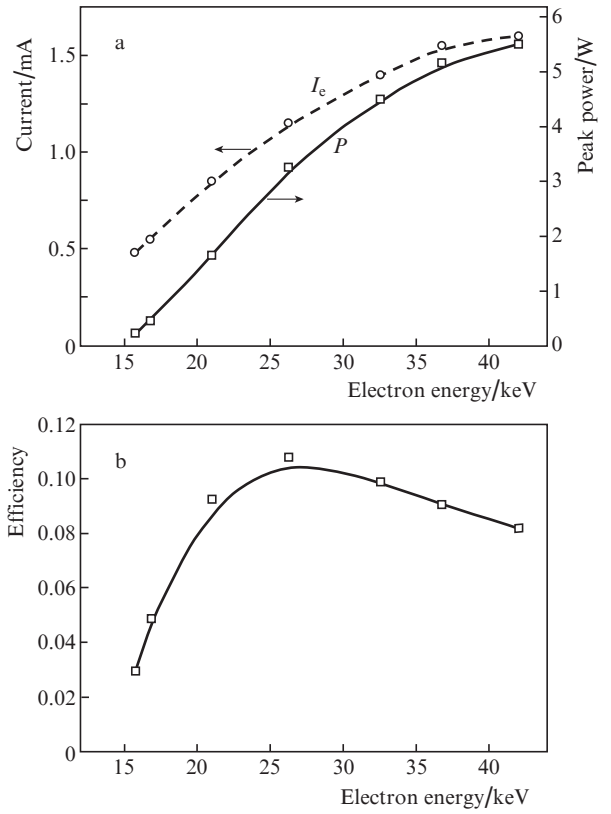

Figure 7. (a) Current and highest output power as well as (b) efficiency of the B-structure SDL as functions of the electron energy.

5. Conclusions

Thus, we have implemented and investigated an electron-beam pumped SDL based on an InGaAs/AlGaAs heterostructures grown by MOCVD. The best of the resultant structures was used to make a pulse-periodic laser operating with an output power of 5.5 W at a wavelength of 1.062 mm.

Acknowledgements. This work was supported by the Russian Foundation for Basic Research (Grant No. 18-02-00436) and the Competitiveness Enhancement Programme of the National Research Nuclear University 'MEPhI' (Agreement No. 02.a03.21.0005).

References

1. Kuznetsov M., Hakimi F., Sprague R., Mooradian A. *IEEE Photon. Technol. Lett.*, **9**, 1063 (1997).
2. Heinen B., Wang T.-L., Sparenberg M., Weber A., Kunert B., Hader J., Koch S.W., Moloney J.V., Koch M., Stolz W. *Electron. Lett.*, **48**, 516 (2012).
3. Shu Q.-Z., Caprara A.L., Berger J.D., Anthon D.W., Jerman H., Spinelli L. *Proc. SPIE*, **7193**, 719319 (2009).
4. Kaneda Y., Wang T.-L., Yarborough J.M., Fallahi M., Moloney J.V., Yoshimura M., Mori Y., Sasaki T. *Proc. SPIE*, **7193**, 719318 (2009).
5. Kozlovsky V.I., Kuznetsov P.I., Sviridov D.E., Yakushcheva G.G. *Quantum Electron.*, **42**, 583 (2012) [*Kvantovaya Elektron.*, **42**, 583 (2012)].
6. Kozlovsky V.I., Okhotnikov O.G., Popov Y.M. *IEEE J. Quantum Electron.*, **49**, 108 (2013).